

Evidence for a multi-level trophic organization of the human gut microbiome

Tong Wang^{1, 2, †}, Akshit Goyal^{3, †}, Veronika Dubinkina^{2, 4}, Sergei Maslov^{2, 4, *}

1 Department of Physics, University of Illinois at Urbana-Champaign, IL 61801, USA

2 Carl R. Woese Institute for Genomic Biology, University of Illinois at Urbana-Champaign, IL 61801, USA

3 Simons Centre for the Study of Living Machines, National Centre for Biological Sciences, Tata Institute of Fundamental Research, Bengaluru 560 065, India

4 Department of Bioengineering, University of Illinois at Urbana-Champaign, IL 61801, USA

† These authors contributed equally to this work.

* Correspondence: maslov@illinois.edu

1 Abstract

2 The human gut microbiome is a complex ecosystem, in which hundreds of microbial species and
3 metabolites coexist, in part due to an extensive network of cross-feeding interactions. However,
4 both the large-scale trophic organization of this ecosystem, and its effects on the underlying
5 metabolic flow, remain unexplored. Here, using a simplified model, we provide quantitative
6 support for a multi-level trophic organization of the human gut microbiome, where microbes
7 consume and secrete metabolites in multiple iterative steps. Using a manually-curated set of
8 metabolic interactions between microbes, our model suggests about four trophic levels, each
9 characterized by a high level-to-level metabolic transfer of byproducts. It also quantitatively
10 predicts the typical metabolic environment of the gut (fecal metabolome) in approximate
11 agreement with the real data. To understand the consequences of this trophic organization, we
12 quantify the metabolic flow and biomass distribution, and explore patterns of microbial and
13 metabolic diversity in different levels. The hierarchical trophic organization suggested by our
14 model can help mechanistically establish causal links between the abundances of microbes and
15 metabolites in the human gut.

16 Introduction

17 The human gut microbiome is a complex ecosystem with several hundreds of microbial species
18 [1, 2] consuming, producing and exchanging hundreds of metabolites [3, 4, 5, 6, 7]. With
19 the advent of high-throughput genomics and metabolomics techniques, it is now possible to
20 simultaneously measure the levels of individual metabolites (the fecal metabolome), as well as
21 the abundances of individual microbial species [8]. Quantitatively connecting these levels with
22 each other, requires knowledge of the relationships between microbes and metabolites in their
23 shared environment: who produces what, and who consumes what? [9, 10] In recent studies,
24 information about these relationships for all of the common species and metabolites in the human
25 gut has been gathered using both manual curation from published studies [6] and automated
26 genome reconstruction methods [3]. This has laid the foundation for mechanistic models which
27 would allow one to relate metabolome composition to microbiome composition [11, 12].

28 More generally, the construction of mechanistic models has been hindered by the complexity
29 of dynamical processes taking place in the human gut, which in addition to cross-feeding and

30 competition, includes differential spatial distribution and species motility, interactions of microbes
31 with host immune system and bacteriophages, changes in activity of metabolic pathways in
32 individual species in response to environmental parameters, etc. This complexity can be tackled
33 on several distinct levels. For 2-3 species it is possible to construct a detailed dynamical model
34 taking into account the spatial organization and flow of microbes and nutrients within the lower
35 gut [13, 14], or optimizing the intracellular metabolic flows as well as competition for extracellular
36 nutrients using dynamic flux balance analysis (dFBA) models [15, 4].

37 For around 10 microbial species, and a comparable number of metabolites, it is possible
38 to construct a Consumer Resource Model (CRM) taking into account microbial competition
39 for nutrients, the generation of metabolic byproducts, and the different tolerance of species to
40 various environmental factors like pH. Using the existing experimental data on consumption and
41 production kinetics of different metabolites, it is possible to fit some (but not all) of around 80
42 parameters in such a model [16].

43 However, modeling 100s of species and metabolites, typically present in an individual's gut
44 microbiome, requires thousands of parameters, which cannot be estimated from the current
45 experimental data. Therefore, any such model must instead resort to a few "global parameters"
46 that appropriately coarse-grain the relevant ecosystem dynamics. Here, we propose such a
47 coarse-grained model of the human gut microbiome, hierarchically organized into several distinct
48 trophic levels. In each level, metabolites are consumed by a subset of microbial species in the
49 microbiome, and partially converted to microbial biomass. A remainder of these metabolites is
50 excreted as metabolic byproducts, which then form the next level of metabolites. The metabolites
51 in this level can then be consumed as nutrients by another subset of microbial species. Our model
52 needs two global parameters: (1) the fraction of nutrients converted to metabolic byproducts
53 by any microbial species, and (2) the number of trophic levels into which the ecosystem is
54 hierarchically organized.

55 While previous studies have suggested that such cross-feeding of metabolic byproducts is
56 common in the microbiome, the extent to which this ecosystem is hierarchically organized has not
57 been quantified. Our model suggests that both, the gut microbiome, and its relevant metabolites,
58 are organized into roughly 4 trophic levels, which interconnect these microbes and metabolites
59 in quantitative agreement with their experimentally measured levels. We also show that this
60 model can predict the flow of biomass and metabolites through these trophic levels, quantify
61 the relative contribution of the observed microbes and metabolites to these levels, and thereby
62 allows us to study how microbial competition and cooperation for nutrients maintain diversity at
63 each level.

64 **Model and Results**

65 **Multi-level trophic model of the human gut microbiome**

66 Our model aims to approximate the metabolic flow through the intricate cross-feeding network of
67 microbes in the lower intestine (hereafter, "gut") human individuals (figure 1A). This flow begins
68 with metabolites entering the gut, which are subsequently consumed and processed by multiple
69 microbial species. We assume that each microbial species grows by converting a certain fraction
70 of its metabolic inputs (nutrients) to its biomass and secretes the rest as metabolic byproducts
71 (figure 1B). We define the byproduct fraction, f , one of the two key parameters of our model, as
72 the fraction of nutrients secreted as byproducts. The complementary biomass fraction, $1 - f$,
73 is the fraction of nutrient inputs converted to microbial biomass. The metabolic byproducts
74 produced from the nutrients entering the gut, can be further consumed by some species in the

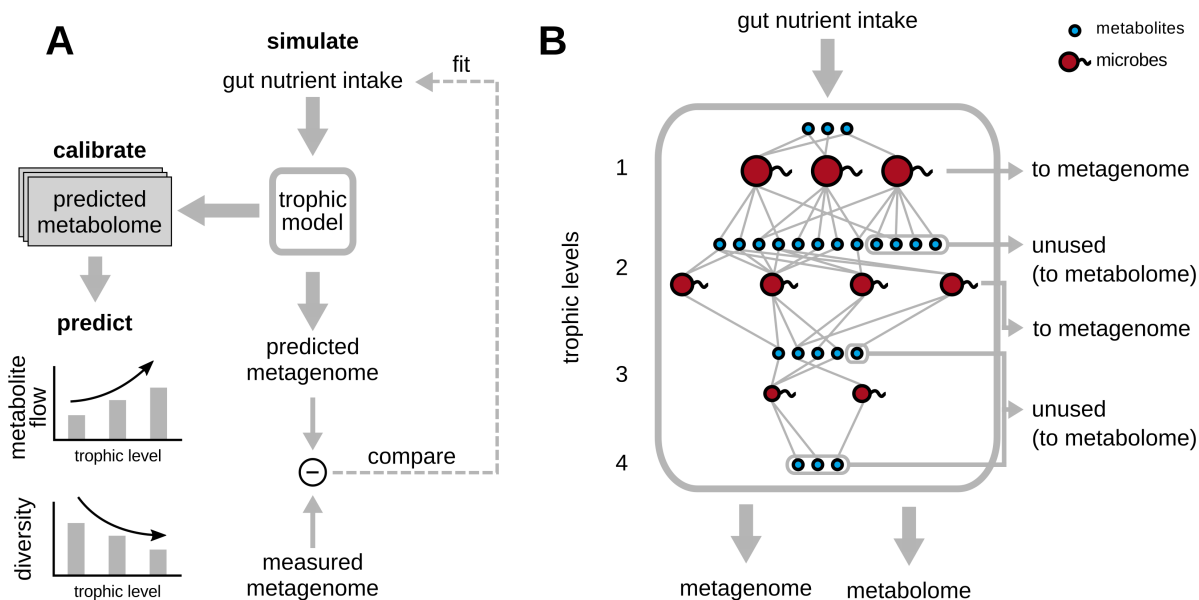


Figure 1: Overview of the trophic model, its calibration and predictions. (A) Schematic diagram showing the various steps in the trophic model, which uses fits the gut nutrient intake profile best approximating the measured metagenome, and outputs a predicted metagenome (microbial abundances) and metabolome. The experimentally measured metabolome is used to calibrate the number of trophic levels, N_ℓ and byproduct fraction, f of the model. (B) “Zoomed-in” view of the trophic model from (A), with different microbial species (red) and metabolites (blue) spread across the four trophic levels suggested by the model. At each level, metabolites are consumed by microbial species, and converted partially to their biomass, while the remainder is secreted as metabolic byproducts, which are nutrients for the next trophic level. Metabolites that are left unconsumed across each level are assumed to eventually exit the gut as part of the fecal metabolome, while the biomass accumulated by each species across all levels contributes to the metagenome.

75 microbiome, in turn generating a set of secondary metabolic byproducts. We call each step of
 76 this process of metabolite consumption and byproduct generation, a trophic level. Due to factors
 77 such as limited gut motility, and a finite length of the lower gut, we assume that this process only
 78 continues for a finite number of levels, N_ℓ , the second key parameter of our model. At the end of
 79 this process, metabolites left unconsumed after passing through N_ℓ trophic levels are assumed to
 80 leave the gut as a part of the feces (figure 1B).

81 In order to quantitatively describe all the steps of this process, our model requires the
 82 following information:

- 83 • The metabolic capabilities of different microbial species in the gut, i.e. which microbes can
 84 consume which metabolites, and secrete which others. For this, we used a manually curated
 85 database connecting 567 common human gut microbes to 235 gut-relevant metabolites they
 86 are capable of either consuming or producing as byproducts [6] (see Methods for details).
- 87 • The nutrient intake to the gut, which is the first set of metabolites that are consumed by
 88 the microbiome. Since the levels of these metabolites in a given individual are generally
 89 unknown, we first curated a list of 19 metabolites likely to constitute the bulk of this
 90 nutrient intake, and subsequently fitted their levels to best describe the observed microbial
 91 abundances in the gut of each individual (see Methods). We collected such microbial
 92 abundance data from various sources, in particular: 380 samples from the large-scale whole-

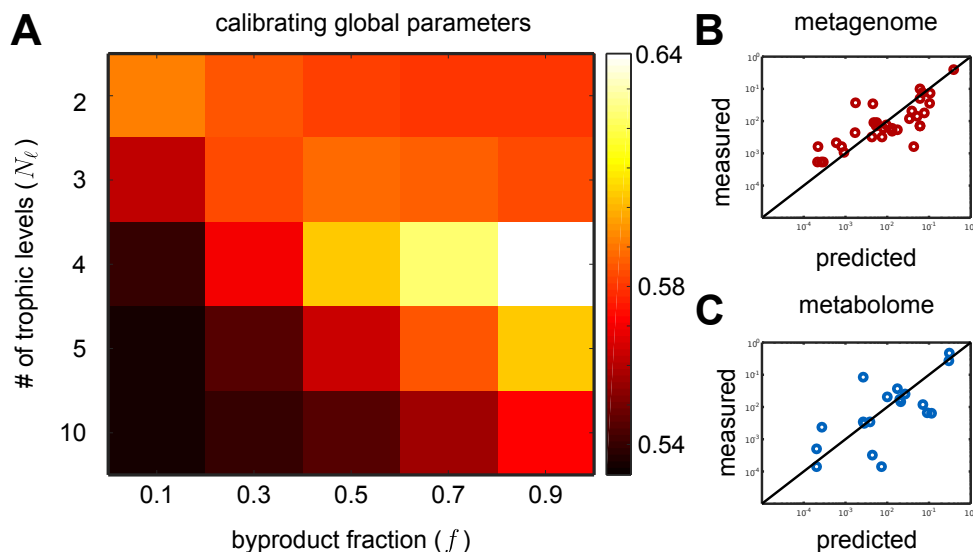


Figure 2: Calibration of the model. (A) Heatmap of the Pearson correlation between experimentally measured and predicted metabolomes for different combinations of parameters f and N_ℓ . The plotted value is the correlation coefficient averaged over 41 individuals in Ref. [18] (B) Comparison between the experimentally observed bacterial abundances in a representative individual (y-axis) and their best fits from our model (x-axis) with $f = 0.9$ and $N_\ell = 4$. (C) Comparison between the experimentally observed fecal metabolome (y-axis) and the predictions of our model (x-axis) with $f = 0.9$ and $N_\ell = 4$ in the same individual shown in panel (B) (Pearson correlation 0.64; P value $< 10^{-5}$).

93 genome sequencing (WGS) studies of healthy individuals (Human Microbiome Project
94 (HMP) [1] and the MetaHIT consortium [2, 17]), 41 samples from a recent 16S rRNA study
95 of 10 year old children in Thailand [18].

- 96 • The kinetics of nutrient uptake and byproduct release, i.e. the rates we refer to as λ 's,
97 at which different microbial species obtain and secrete different metabolites in the gut
98 environment. Since this information is unknown for most of our microbes and metabolites,
99 we made some simplifying assumptions. We assumed that, in a given level, when species
100 consume the same metabolite, they receive it in proportion to their abundance in the
101 microbiome. When secreting metabolic byproducts, we assumed equal splitting, such that
102 every metabolite secreted by a given species was released in the same fraction. However,
103 we later verified that the predictions of our model was relatively insensitive to the exact
104 values of these parameters, by repeating our simulations with randomized values of these
105 parameters (see figure S1).

106 Calibrating the key parameters of the model

107 To calibrate the two key parameters of our model, f and N_ℓ , we used data from the 41 individuals
108 from a recent 16S rRNA sequencing study of Thai children [18] for which both, 16S rRNA
109 metagenomic profiles, as well as quantitative levels of 214 metabolites in the fecal metabolome,
110 were available. In each individual we fitted the nutrient intakes of the 19 metabolites to best agree
111 with experimental microbial abundances. A representative example comparing the predicted and
112 measured bacterial abundances is shown in Fig. 2B. The Pearson correlation coefficient for data
113 shown in this plot is 0.94, while in individual participants it ranged between 0.81 ± 0.17 .

114 We carried out these fits of microbial abundances for each of the 41 individuals studied in

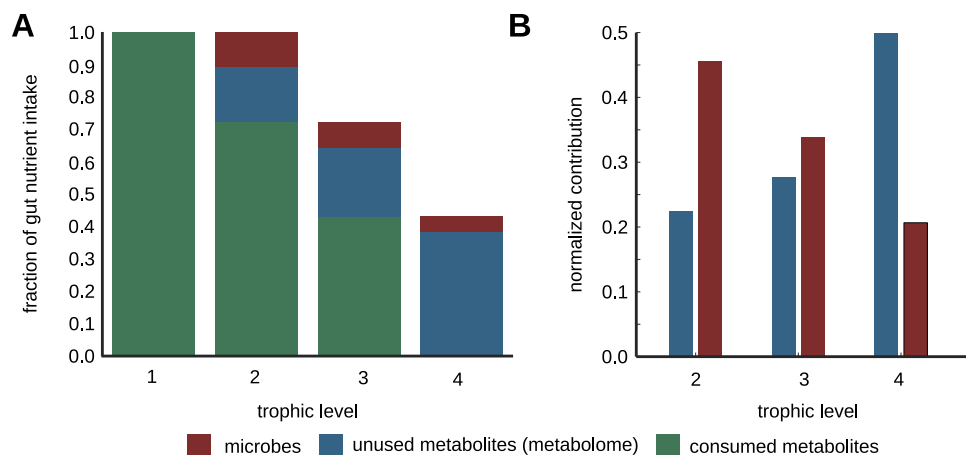


Figure 3: Metabolite and biomass flow through the levels. (A) Cascading nature of nutrient flow across trophic levels: nutrient intake to the gut (the leftmost turquoise bar) is gradually converted into microbial biomass (red bars in each level) and metabolic byproducts (turquoise bars in each level). Some fraction of these byproducts (blue bars in each level) cannot be consumed by the microbiome and hence remains further unprocessed until it leaves an individual as their fecal metabolome. The metabolic byproducts of each level (turquoise bars) serve as the nutrient intake for microbes in the next level. The process ends at level 4 where all byproducts remain unconsumed thereby enter the fecal metabolome. (B) Normalized contribution of of the nutrient intake to microbial biomass (red) and fecal metabolome (blue) split across levels 2 to 4. Dashed lines show that consumable metabolites generated at a previous level serve as metabolic inputs to the next level.

115 Ref. [18] for a broad range of two parameters of our model - the byproduct fraction f ranging
116 between 0.1 and 0.9 and the number of trophic levels N_ℓ between 2 and 10. For each individual
117 and each pair of parameters f and N_ℓ we used our model to predict the fecal metabolome
118 profile. This predicted metabolome was subsequently compared to the experimental data of Ref.
119 [18] measured in the same individual. Around 19 of our predicted metabolites (variable across
120 individuals) were actually among the ones experimentally measured in Ref. [18]. The quality
121 of this comparison was quantified using the Pearson correlation coefficient (see Fig. 2A). The
122 model with parameters $f = 0.9$ and $N_\ell = 4$ best agrees with the experimental data (Pearson
123 correlation 0.7 ± 0.2 ; median P value 8×10^{-4}) compared with all other values we tried. Hence,
124 we used this combination of parameters in all subsequent simulations of our model.

125 We found predicted and experimental observed metabolic profiles to be in reasonable agreement
126 with each other. Fig. 2C shows the predicted and observed fecal metabolome data plotted against
127 each other for the same individual used in Fig. 2B. Note that, while the agreement between the
128 observed and predicted microbial abundances shown in Fig. 2B is the outcome of our fitting the
129 levels of intake metabolites, the fecal metabolome is an independent prediction of our model. It
130 naturally emerges from the trophic organization of the metabolic flow and agrees well with the
131 experimentally observed metabolome. Thus our simplified model supports the organization of
132 the microbiome into roughly four trophic levels with byproduct fraction around 0.9.

133 Predictions of the multi-level trophic model

134 Metabolite and biomass flow through trophic levels

135 With a well-calibrated and tested model we are now in a position to apply it to a broader set
136 of human microbiome data. To this end we chose data for 380 healthy adult individuals from

137 several countries (Europe [2], USA [1], and China [17]). For each individual, we used our model
138 to predict its metabolome (that has not been measured experimentally) and quantified the flow
139 of nutrients (or metabolic activity) through 4 trophic levels in our model averaged over these
140 individuals.

141 Fig. 3A shows the cascading nature of this flow: metabolites enter the gut as nutrient intake
142 shown as the leftmost turquoise bar in Fig. 3A. Roughly, a fraction $1 - f = 0.1$ of this nutrient
143 intake is converted into microbial biomass (red bar), while the remaining fraction $f = 0.9$ is
144 excreted as metabolic byproducts. Some fraction of these metabolic byproducts (blue bar) cannot
145 be consumed by any of the microbes in individuals microbiome and hence ultimately it leaves the
146 individual as part of their fecal metabolome. The metabolic byproducts that can be consumed
147 by the microbiome (turquoise bar) serve as the nutrient intake for microbes in the next level (i.e.
148 level 3). This scenario repeats itself over the next levels until the level 4, beyond which we assume
149 all the byproducts enter the fecal metabolome. Note that, even though some of these byproducts
150 can be consumed by gut microbes, our previous calibration (Fig. 2A) suggests that this does
151 not happen. We believe this may be due to the finite time of flow of nutrients through the gut.
152 Fig. 3B shows the normalized contributions of the nutrient intake to microbial biomass (red)
153 and fecal metabolome (blue) split across trophic levels. We observe a contrasting pattern across
154 levels, with the contribution to microbial biomass decreasing along levels, whereas the fraction
155 of unused metabolites (contribution to the fecal metabolome) increases. It is also worth noting
156 that the same microbial and metabolic species get contributions from multiple trophic levels,
157 i.e. the same microbes that consume nutrients and excrete byproducts in earlier levels can also
158 grow on metabolites generated in later levels. Thus, even though the dominant contribution to a
159 species' biomass is typically derived from a specific trophic level, species can grow by consuming
160 metabolites from multiple levels.

161 **Quantifying diversity across trophic levels**

162 The diversity of microbial communities can be separately defined both phylogenetically and
163 functionally. Phylogenetic diversity counts the number of abundant microbial species inferred
164 from the metagenomic profile. On the other hand, functional diversity quantifies the variety
165 of collective metabolic activities of these species, which in our case could be inferred from the
166 metabolome profile. Our model allows to quantify both types of diversity on a level-by-level
167 basis. Instead of just calculating the presence or absence of microbial species or metabolites at
168 each level, we weighed each microbe or metabolite by their relative contribution to the metabolic
169 activity at that trophic level. At each level, we calculated the effective α -, β - and γ -diversity,
170 separately for microbes and metabolites (see Methods for details).

171 Fig. 4 shows the effective α -, β - and γ - diversity for microbes (grouped at the species
172 and genus levels) and metabolites, averaged over our 380 healthy individuals. The microbes
173 first appear in the second trophic level feeding off the nutrient intake metabolites in the first
174 level. We found that the α -diversity (the average number of abundant entities weighted by their
175 contribution to each level) systematically increases with the level number for both microbes
176 and metabolites. There is no clear trend in the γ -diversity of microbes grouped at the species
177 level (the “pan-microbiome” diversity, i.e. the number of abundant species in the combined
178 metagenomes of 380 individuals).

179 Finally the beta-diversity of microbial species, defined as the ratio between γ - and α -diversity
180 is the highest (~ 4) in the first level, while being considerably lower (~ 2.5) in the next two
181 levels. The β -diversity addresses the following important question: how variable are the abundant
182 species between individuals?

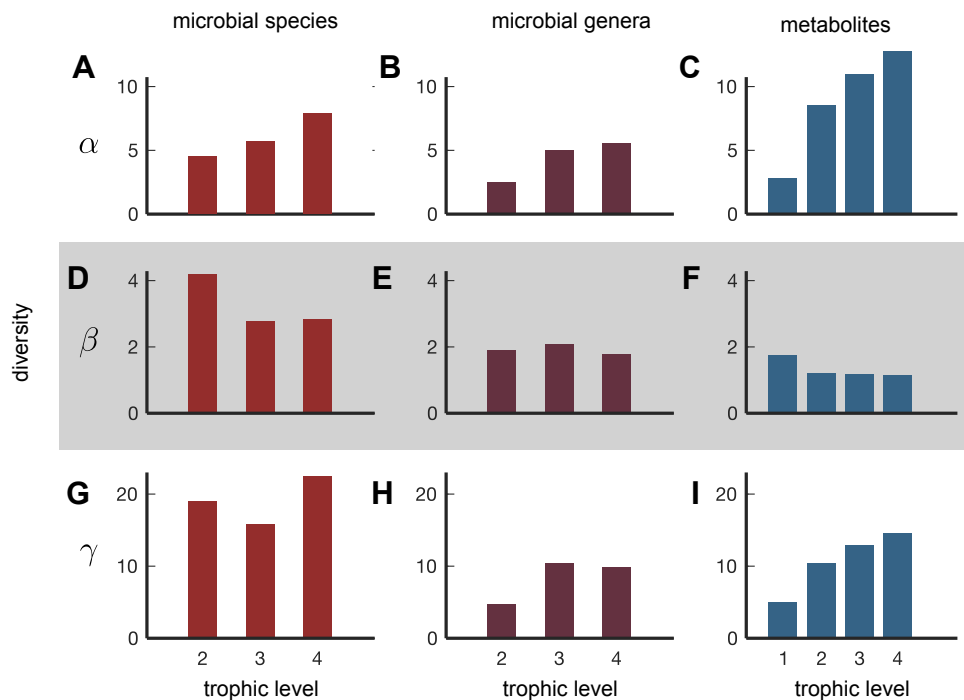


Figure 4: Metabolite and microbial diversity at different levels. Effective (A–C) α -diversity, (D–F) β -diversity, (G–I) γ -diversity in microbial species (A, D, G), microbial genera (B, E, H), and metabolites (C, F, I) plotted as a function of trophic level (1–4) and averaged across 380 individuals.

183 While we found that the β -diversity of microbial species could be as large as 4 (Fig. 4), when
184 we grouped organisms by their genus, β diversity decreased down to ~ 2 across all levels (Fig.
185 4E). This drop in β -diversity was the most pronounced in the uppermost trophic level. The
186 overall reduction of β -diversity shown in Fig. 4E relative to Fig. 4D suggests that the chief
187 driver of species variability in the gut microbiome is within-genus competition. Such a pattern
188 has previously been explained by a “lottery-like” process of microbial competition within the gut
189 [19].

190 We also quantified the diversity of metabolites across 4 trophic levels. We found that the β
191 diversity of metabolites was the highest in the uppermost level of nutrients (~ 2) and lower in
192 the next three levels (~ 1). While this declining trend was similar to that observed for microbial
193 diversity, surprisingly, the value of β diversity for nutrients was much smaller than for microbes
194 (about 2.5 times lower across all levels). This suggests the picture of functional stability — in
195 spite of taxonomic variability — in all trophic levels of the human gut microbiome, namely
196 that even though the species composition of the microbiome can be quite different for different
197 individuals, their metabolic function is quite similar. These results supplement similar findings of
198 the HMP project [1] by breaking them up into trophic levels and by using metabolome diversity
199 instead of metabolic pathways diversity to quantify the extent of functional similarity.

200 Discussion

201 Above we introduced and studied a mechanistic, consumer-resource model of the human gut
202 microbiome quantifying the flow of metabolites and the gradual building up of microbial biomass
203 across several trophic levels. What distinguishes our model is its ability to simultaneously capture

204 the metabolic activities of hundreds of species consuming and producing hundreds of metabolites.
205 Using only the metabolic capabilities — who eats what, and makes what — of different species in
206 the microbiome, we uncovered roughly four trophic levels in the human gut microbiome. At each
207 of these levels, some microbes consume nutrients, and convert them partially to their biomass,
208 while the remainder gets secreted as metabolic byproducts. These metabolic byproducts can
209 then serve as nutrients for microbes in the next trophic level.

210 Understanding such a trophic organization of microbial ecosystems is important because it
211 helps identify causal relationships between microbes and metabolites at two consecutive trophic
212 levels and helps to separate them from purely correlative connections, either at the same or at
213 more distant levels. Thus it extends the previously introduced concept of a “microbial metabolic
214 influence network” [6] by highlighting its hierarchical structure in which species/metabolites
215 assigned to higher trophic levels could affect a large number of species/metabolites located
216 downstream from them. The concept of trophic levels is widely discussed in macroecology helping
217 to make sense of flow of nutrients and energy in large food webs, but rarely highlighted in the
218 microbial ecosystems literature.

219 Our model also allows us to quantify the diversity of both species and metabolites contributing
220 to different trophic levels. One conclusion we made was that the functional convergence of the
221 microbiome holds roughly equally across all trophic levels. Indeed, at each level we observed
222 the microbial diversity across different individuals was considerably higher than their metabolic
223 diversity. Our model also provides additional support to the “lottery” scenario described in Ref.
224 [19], especially in the first trophic level. According to this scenario, there are multiple species
225 nearly equally capable of occupying a certain ecological niche, which in our model corresponds
226 to the set of nutrients they consume and secrete as byproducts. The first species to occupy this
227 niche prevents equivalent microbes from entering it. This is reflected in a high β -diversity of
228 microbial species combined with a low to moderate β -diversity of microbial genera to which they
229 belong and low β -diversity of their metabolic byproducts.

230 The flow of metabolites through the species-to-species cross-feeding network is reminiscent of
231 the flow of web traffic modeled by Google’s original PageRank algorithm [20]. In the PageRank
232 algorithm, each web page redirects $f = 0.85$ of its traffic along hyperlinks to other web pages
233 thereby contributing to their network traffic. Interestingly, in our model, each bacterial species
234 redistributes or converts a fraction $f = 0.9$ of its nutrients to other byproducts, which is close to
235 that found by Page and Brin for web traffic [20].

236 Our model is focused on studying the effects of cross-feeding and competition of different
237 microbes for their nutrients. Thereby it ignores a number of important factors known to impact
238 the composition of the human gut microbiome. These include interactions with host and its
239 immune system [21] as well as with viruses [22], and environmental parameters other than
240 nutrients, such as pH [14], spatial organization [23], etc. Instead, our model uses only two
241 adjustable parameters: the byproduct fraction f and the number of trophic levels N_ℓ , assumed
242 to be common to all species. This very small number of parameters has been a conscious choice
243 on our part. We are perfectly aware that species differ from each other in their byproduct ratios,
244 and that the metabolic flows are not equally split among multiple byproducts. This can be
245 easily captured by a variant of our model in which different nutrient inputs and and byproduct
246 outputs of a given microbial species are characterized by different kinetic rates. However, this
247 would immediately increase the number of parameters from 2 to more than 3,600. To calibrate a
248 model with such a huge number of parameters one needs many more experimental data than
249 we have access to right now. However, we tested the sensitivity of our model to variation in
250 these parameters by repeating our simulations for 100 random sets of nutrient kinetic uptake
251 and byproduct release rates (λ 's in our model), and found that this did not qualitatively change

252 our central result (i.e. that the human gut microbiome is composed of roughly $N_\ell = 4$ trophic
253 levels with a byproduct fraction $f = 0.9$). Surprisingly, our metabolome predictions were also
254 relatively insensitive with respect to varying these parameters (Figure S1). The exact nature
255 of the robustness of these metabolome predictions is beyond the scope of this paper, and the
256 subject of future work.

257 Methods

258 Obtaining data for microbial metabolic capabilities

259 For information about the metabolic capabilities of human gut microbes, we adopted a recently
260 published manually-curated database, NJS16, which includes such data for 570 common gut
261 microbial species and 244 relevant metabolites from Ref. [6]. This database recorded, for each
262 microbial species, which metabolites each of the species could consume, and which they secreted
263 as byproducts. Since we were interested in those metabolites that could be used for microbial
264 growth, we removed metabolites such as ions (e.g. Na^+ , Ca^+) from NJS16. Moreover, we
265 constrained our analyses to microbes only, and therefore removed the 3 types of human cells from
266 NJS16. This left us with a database with 567 microbes, 235 metabolites and 4,248 interactions
267 connecting these microbes with corresponding metabolites (see table S1 for the complete table of
268 interactions).

269 Obtaining metagenomic and metabolomic data

270 To calibrate the key parameters of our model, we used a previously published dataset, namely a
271 16S rRNA sequencing study of 41 human individuals from rural and urban areas in Thailand
272 [18]. From these data, we collected the reported 16S rRNA OTU abundances as well as their
273 corresponding taxonomy. We explicitly removed all OTUs that did not have an assigned species-
274 level taxonomy. The remaining OTUs explained roughly 71% ($\pm 15\%$) of the bacterial abundances
275 per sample.

276 We then mapped these species names to species names listed in the NJS16 database. We
277 found an exact match for 110 species out of 208 in this table. In order to improve the species
278 coverage from the abundance data, we manually mapped the remaining species in the following
279 manner. For those genera in NJS16, whose member species had identical metabolic capabilities,
280 we assumed that the capabilities of other, unmapped species from these genera were the same
281 as these species. For several well-studied bacterial genera, such as *Bacteroides*, we determined
282 a “core” set of metabolic capabilities (i.e. those metabolites that could either be consumed
283 or secreted by all species in that genus), and assigned them to all unmapped species in that
284 genus (i.e. those with known abundances, but otherwise understudied metabolic capabilities in
285 NJS16). This allowed us to map an additional 20 microbial species from the abundance data,
286 and incorporate into our model. Note that we did this additional mapping, only for those genera,
287 where species metabolic capabilities were identical.

288 To quantify the metabolome levels in each individual, we used the available quantitative
289 metabolome profiles (obtained via from CE-TOF MS) corresponding to the 41 individuals whose
290 metagenomic samples we had. Here, we mapped the reported metabolites to our database of
291 metabolic capabilities using KEGG identifiers, which revealed 84 such measured metabolites.

292 To make predictions about metabolic flow and effective diversity from our model, we used
293 additional metagenomic datasets, namely those from the Human Microbiome Project (HMP) [1]
294 and MetaHIT [2, 17], for which we had microbial abundances, but no fecal metabolome. This

295 resulted in an additional 380 human individuals, for which we obtained tables of MetaPhlAn2
296 microbial abundances, and mapped species names to those in NJS16 using the same procedure
297 described above. Here, out of a total of 532 microbial species detected over these data, we could
298 map and incorporate 316 species. Of these, 207 were mapped through an exact taxonomic match,
299 and 109 by a genus-capability match. These incorporated species covered, on average, 90% of
300 the total microbial abundance in each individual sample.

301 **Determining the components of the nutrient intake to the gut**

302 The inputs of our model are the relative abundances of microbial species in each individual,
303 which are known (and described above), and the levels of various nutrients reaching their lower
304 gut, which we fit using the model. For simplicity, we do not explicitly include the various
305 polysaccharides (dietary fibers, starch, etc.) known to constitute the bulk of an individual's diet.
306 Instead, we chose not to include the polysaccharides themselves, but instead use their breakdown
307 products as the direct nutrient intake to the gut. The reason for this is our limited quantitative
308 understanding of the processes by which these polysaccharides are converted to these breakdown
309 products, e.g. the levels of extracellular enzymes, variability in their composition (their lability),
310 etc. This curated nutrient intake consisted of 19 metabolites, such as arabinose, raffinose, and
311 xylose (see table S2 for the complete list of metabolites).

312 **Simulating the trophic model**

313 For a specific individual, our model comprises multiple iterative “rounds” of metabolite con-
314 sumption by microbes and the subsequent generation of metabolic byproducts, with each round
315 constituting a trophic level. At each level, all metabolites produced in the previous level could
316 be consumed by all microbial species detected in the specific individual's gut. Note that at the
317 first level, these metabolites were given by the nutrient intake to the gut, as described above.
318 Any metabolite that could be consumed by multiple microbial species, was split across those
319 species in proportion to their measured relative abundances. Those metabolites that could
320 not be consumed at any level were assumed to eventually exit the gut, and form part of the
321 individual's fecal metabolome. Upon metabolite consumption in any trophic level, we assumed
322 that all microbial species that consumed these metabolites, converted a fraction $(1 - f)$ of the
323 total consumed metabolites to their biomass. The remaining fraction, f (assumed fixed for all
324 species) was converted to byproducts for the next level. Here, we assumed that each of the
325 species produced all the byproducts it was capable of in equal amounts. After N_ℓ such iterative
326 rounds (calibrated separately, see the next section), we assumed that this process ends. We
327 added up all the biomass accumulated by each microbial species across all trophic levels as their
328 total biomass, and added up all the unconsumed metabolite levels as the total fecal metabolome.
329 Finally, we normalized, both the microbial biomass and metabolite amounts separately, to obtain
330 the relative microbial abundances and relative metabolome profiles, respectively.

331 **Fitting and inferring the nutrient intake to the gut**

332 Simulating the model required us to know the nutrient intake to the gut, for which there are
333 no available experimental measurements. Therefore, we inferred the amounts of these 19 intake
334 metabolites by fitting the microbial abundances predicted by our model with those measured
335 from each individual's microbiome. We used a nonlinear optimization technique (implemented
336 as `lsqnonlin` in MATLAB R2018a, Mathworks Inc.) for this fit, from which we obtained the
337 amounts of the gut nutrient intake supplied to the first trophic level, that minimized the sum of

338 squares of the logarithm of the difference between the observed species abundances, and those
339 predicted by our model. Typically, we fit 19 metabolite amounts for each human individual, who
340 had roughly 80 microbial species.

341 **Calculating level-by-level diversity**

To quantify the diversity of microbes and metabolites at each trophic level across the 380 individuals we studied, we used three measures popular in the ecosystems literature: namely the α -, β - and γ - diversity [24, 25, 26]. For each individual, we calculated the α -diversity of microbes and metabolites on each of the trophic levels. For this we first quantified the relative contributions of a given level to microbial abundances, and separately to the fecal metabolome profile. The contribution of a given trophic level ℓ to the relative abundance of a species (microbial or, separately, metabolic) i in a specific individual j is given by $p_i(\ell, j)$ normalized by $\sum_{i=1}^S p_i(\ell, j) = 1$. The α -diversity

$$D_\alpha(\ell) = \frac{1}{\langle \sum_{i=1}^S p_i(\ell, j)^2 \rangle_j},$$

342 where $\langle \cdot \rangle_j$ represents taking the average across 380 individuals used in our analysis.

343 Across all individuals, we calculated the γ -diversity of microbes and metabolites in their gut,
344 which quantified the “global” diversity across all individuals, as:

$$D_\gamma(\ell) = \frac{1}{\sum_{i=1}^S p_i(\ell)^2},$$

345 where $p_i(\ell) = \langle p_i(\ell, j) \rangle_j$ is the mean relative abundance of species (or metabolite) i at the trophic
346 level ℓ across all individuals used in our analysis.

347 Finally, to quantify the between-individual variability in microbial and metabolite diversity,
348 we calculated the overall β -diversity, which is the ratio of the global to local diversity, as:

$$D_\beta(\ell) = \frac{D_\gamma(\ell)}{D_\alpha(\ell)}.$$

349 **Code availability**

350 All computer code and extracted data files used in this study are available at the following URL:
351 https://github.com/eltanin4/trophic_gut.

352 **Supplementary Figures and Tables**

353 **Figure S1 Effect of changing kinetic parameters on model prediction.** Scatter plot
354 of the measured and predicted metabolome where, instead of considering equal specific nutrient
355 uptake and byproduct release rates, λ 's in our model, we take several random sets (in black).
356 Error bars (in black) indicate standard deviation in the predicted levels of specific metabolites
357 for different sets of λ 's. The solid line represents $x = y$. Red squares indicate the predicted
358 metabolome for the default set of kinetic parameters used, i.e. when all of λ 's were set equal to 1.

359 **Table S1 Microbial and metabolite interactions used in the model.** Table of all 4,248
360 interactions between microbes and metabolites used in the model, from Ref. [6].

361 **Table S2 Components of the nutrient intake to the gut.** List of all 19 metabolites used
362 to fit the gut nutrient intake in the model.

363 Acknowledgments

364 A.G. acknowledges support from the Simons Foundation and the American Physical Society. We
365 thank Parth Pratim Pandey for useful discussions.

366 Conflicts of interest

367 The authors declare that there are no competing interests.

References

- [1] Consortium HMP, et al. Structure, function and diversity of the healthy human microbiome. *Nature*. 2012;486(7402):207–214.
- [2] Qin J, Li R, Raes J, Arumugam M, Burgdorf KS, Manichanh C, et al. A human gut microbial gene catalogue established by metagenomic sequencing. *nature*. 2010;464(7285):59–65.
- [3] Magnúsdóttir S, Heinken A, Kutt L, Ravcheev DA, Bauer E, Noronha A, et al. Generation of genome-scale metabolic reconstructions for 773 members of the human gut microbiota. *Nature biotechnology*. 2017;35(1):81.
- [4] San Roman M, Wagner A. An enormous potential for niche construction through bacterial cross-feeding in a homogeneous environment. *PLoS computational biology*. 2018;14(7):e1006340.
- [5] Pacheco AR, Moel M, Segre D. Costless metabolic secretions as drivers of interspecies interactions in microbial ecosystems. *Nature communications*. 2019;10(1):103.
- [6] Sung J, Kim S, Cabatbat JJT, Jang S, Jin YS, Jung GY, et al. Global metabolic interaction network of the human gut microbiota for context-specific community-scale analysis. *Nature communications*. 2017;8:15393.
- [7] Goyal A. Metabolic adaptations underlying genome flexibility in prokaryotes. *PLoS genetics*. 2018;14(10):e1007763.
- [8] Ponomarova O, Patil KR. Metabolic interactions in microbial communities: untangling the Gordian knot. *Current opinion in microbiology*. 2015;27:37–44.
- [9] Muller EE, Faust K, Widder S, Herold M, Arbas SM, Wilmes P. Using metabolic networks to resolve ecological properties of microbiomes. *Current Opinion in Systems Biology*. 2018;8:73–80.
- [10] Bauer E, Thiele I. From network analysis to functional metabolic modeling of the human gut microbiota. *MSystems*. 2018;3(3):e00209–17.
- [11] Magnúsdóttir S, Thiele I. Modeling metabolism of the human gut microbiome. *Current opinion in biotechnology*. 2018;51:90–96.

- [12] Garza DR, Verk MC, Huynen MA, Dutilh BE. Towards predicting the environmental metabolome from metagenomics with a mechanistic model. *Nature microbiology*. 2018; p. 1.
- [13] Cremer J, Segota I, Yang Cy, Arnoldini M, Sauls JT, Zhang Z, et al. Effect of flow and peristaltic mixing on bacterial growth in a gut-like channel. *Proceedings of the National Academy of Sciences*. 2016;113(41):11414–11419.
- [14] Cremer J, Arnoldini M, Hwa T. Effect of water flow and chemical environment on microbiota growth and composition in the human colon. *Proceedings of the National Academy of Sciences*. 2017;114(25):6438–6443.
- [15] Varma A, Palsson BO. Stoichiometric flux balance models quantitatively predict growth and metabolic by-product secretion in wild-type *Escherichia coli* W3110. *Appl Environ Microbiol*. 1994;60(10):3724–3731.
- [16] Kettle H, Louis P, Holtrop G, Duncan SH, Flint HJ. Modelling the emergent dynamics and major metabolites of the human colonic microbiota. *Environmental microbiology*. 2015;17(5):1615–1630.
- [17] Qin J, Li Y, Cai Z, Li S, Zhu J, Zhang F, et al. A metagenome-wide association study of gut microbiota in type 2 diabetes. *Nature*. 2012;490(7418):55.
- [18] Kisuse J, La-ongkham O, Nakphaichit M, Therdtatha P, Momoda R, Tanaka M, et al. Urban diets linked to gut microbiome and metabolome alterations in children: A comparative cross-sectional study in Thailand. *Frontiers in microbiology*. 2018;9.
- [19] Verster AJ, Borenstein E. Competitive lottery-based assembly of selected clades in the human gut microbiome. *Microbiome*. 2018;6(1):186.
- [20] Page L, Brin S, Motwani R, Winograd T. The PageRank citation ranking: Bringing order to the web. *Stanford InfoLab*; 1999.
- [21] Nicholson JK, Holmes E, Kinross J, Burcelin R, Gibson G, Jia W, et al. Host-gut microbiota metabolic interactions. *Science*. 2012;336(6086):1262–1267.
- [22] Manrique P, Bolduc B, Walk ST, van der Oost J, de Vos WM, Young MJ. Healthy human gut phageome. *Proceedings of the National Academy of Sciences*. 2016;113(37):10400–10405.
- [23] Tropini C, Earle KA, Huang KC, Sonnenburg JL. The gut microbiome: connecting spatial organization to function. *Cell host & microbe*. 2017;21(4):433–442.
- [24] Whittaker RH. Evolution and measurement of species diversity. *Taxon*. 1972; p. 213–251.
- [25] Tuomisto H. A diversity of beta diversities: straightening up a concept gone awry. Part 1. Defining beta diversity as a function of alpha and gamma diversity. *Ecography*. 2010;33(1):2–22.
- [26] Tuomisto H. A consistent terminology for quantifying species diversity? Yes, it does exist. *Oecologia*. 2010;164(4):853–860.

Supplementary Figures

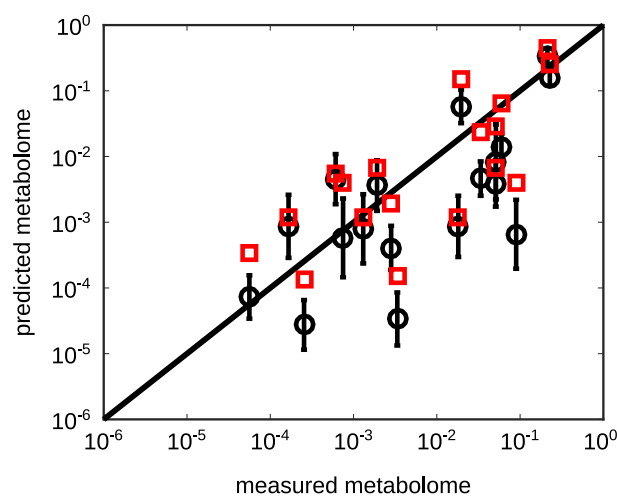


Figure S1: Effect of changing kinetic parameters on model prediction. Scatter plot of the measured and predicted metabolome where, instead of considering equal specific nutrient uptake and byproduct release rates, λ 's in our model, we take several random sets (in black). Error bars (in black) indicate standard deviation in the predicted levels of specific metabolites for different sets of λ 's. The solid line represents $x = y$. Red squares indicate the predicted metabolome for the default set of kinetic parameters used, i.e. when all of λ 's were set equal to 1.